Complex Activation is More Focal and Concentrated to Parenchymal Tissue

Daniel B. Rowe

Department of Biophysics, Medical College of Wisconsin

INTRODUCTION

In functional magnetic resonance imaging, voxel time courses after "image reconstruction" are complex valued. Nearly all fMRI studies derive functional "activation" based on magnitude-only data time courses [1]. The phase time courses are usually discarded. Recently a magnitude activation from complex data model was introduced that did not lose activation power as the SNR decreased [2]. Subsequently the magnitude-only data model activation statistic was derived from complex data [3] and the parameters of both models characterized [4].

MODEL

In a voxel, the observed complex-valued data can be described with the vector/matrix model

$$y = \begin{pmatrix} X & 0 \\ 0 & X \end{pmatrix} \begin{pmatrix} \beta\cos\theta \\ \beta\sin\theta \end{pmatrix} + \eta$$

$$2n\times 1 \qquad 2n\times 2(q+1) \quad 2(q+1)\times 1 \qquad 2n\times 1$$

where the $2n\times 1$ vector $y=(y_R',y_I')'$ is the $n\times 1$ vector of observed real components stacked on the $n\times 1$ vector of observed complex components, X is the $n\times(q+1)$ design matrix, β is the $(q+1)\times 1$ vector of regression coefficients, θ is the 1×1 phase angle, and the vector $\eta=(\eta_R',\eta_I')'$ is the $n\times 1$ vector of real component errors stacked on the $n\times 1$ vector of complex component errors. Functional activation is by testing voxelwise hypothesis such as

$$H_0: C\,\beta = 0 \text{ vs } H_1: C\,\beta \neq 0.$$

The likelihood is maximized under the unconstrained alternative and under the constrained null hypothesis to produce the below hat and tilde estimates respectively.

$$\hat{\theta} = \frac{1}{2}\tan^{-1}\left[\frac{\hat{\beta}_R(X'X)\hat{\beta}_I}{(\hat{\beta}_R(X'X)\hat{\beta}_R - \hat{\beta}_I(X'X)\hat{\beta}_I)/2}\right]$$

$$\hat{\beta} = \cos(\hat{\theta})\hat{\beta}_R + \sin(\hat{\theta})\hat{\beta}_I$$

$$\hat{\sigma}^2 = \frac{1}{2n}\left[y - \begin{pmatrix} X\hat{\beta}\cos\hat{\theta} \\ X\hat{\beta}\sin\hat{\theta} \end{pmatrix}\right]'\left[y - \begin{pmatrix} X\hat{\beta}\cos\hat{\theta} \\ X\hat{\beta}\sin\hat{\theta} \end{pmatrix}\right]$$

$$\tilde{\theta} = \frac{1}{2}\tan^{-1}\left[\frac{\tilde{\beta}_R\Psi(X'X)\tilde{\beta}_I}{(\tilde{\beta}_R\Psi(X'X)\tilde{\beta}_R - \tilde{\beta}_I\Psi(X'X)\tilde{\beta}_I)/2}\right]$$

$$\tilde{\beta} = \cos(\tilde{\theta})\Psi\hat{\beta}_R + \sin(\tilde{\theta})\Psi\hat{\beta}_I$$

$$\tilde{\sigma}^2 = \frac{1}{2n}\left[y - \begin{pmatrix} X\tilde{\beta}\cos\tilde{\theta} \\ X\tilde{\beta}\sin\tilde{\theta} \end{pmatrix}\right]'\left[y - \begin{pmatrix} X\tilde{\beta}\cos\tilde{\theta} \\ X\tilde{\beta}\sin\tilde{\theta} \end{pmatrix}\right]$$

$$\hat{\beta}_R = (X'X)^{-1}X'y_R, \quad \hat{\beta}_I = (X'X)^{-1}X'y_I,$$

$$\Psi = I_{q+1} - (X'X)^{-1}C'[C(X'X)^{-1}C']^{-1}C.$$

The generalized likelihood ratio test λ is formed where the ratio of null and alternative hypothesis estimates inserted into the likelihoods of the numerator and denominator respectively. The test statistic

$$-2\log\lambda = 2n\log\left(\frac{\tilde{\sigma}^2}{\hat{\sigma}^2}\right)$$

is formed in each voxel that is chi-squared distributed in large samples.

CORRESPONDENCE
Daniel B. Rowe, Ph.D.
Department of Biophysics
Medical College of Wisconsin
8701 Watertown Plank Road
Milwaukee, WI 53226
dbrowe@mcw.edu

EXAMPLE

Single subject data was obtained from a block design bilateral finger tapping experiment with 16s off followed by 8 epochs of 16s on and 16s off. A 1.5T GE Signa was used single shot full *k*-space where 5 axial slices of 96×96 acquired reconstructed to 128×128. Voxels were 1.5625×1.5625mm in plane and 5mm thick with TE=47ms and TR=1s where n=272 observations taken. The first 3 observations were deleted followed by low frequency and respiration filtering. A single axial slice of data was selected for analysis. The complex regression model was fit with an intercept, time trend, and ±1 reference function that mimicked the timing of experiment. Activation was computed with the -2log λ chi-squared statistic and Bonferroni thresholded [5].

a) Magnitude-only data activation

b) Phase-only data activation

c) Complex data activation
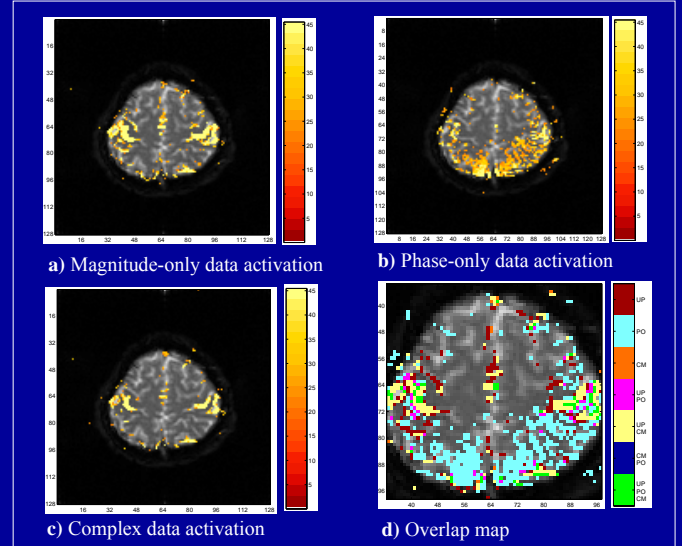
d) Overlap map

In **a)** is the map from magnitude-only data, **b)** from phase-only data, **c)** from complex data, and **d)** a zoomed in colored overlap map of above threshold voxels. Note that the complex data activation pattern is more localized with the complex data model than the magnitude-only data model. In **d)**, voxels that are only above the threshold for the magnitude-only data model are red, only for the phase-only data model light blue, only for the complex data model orange, for the magnitude-only and phase-only data models pink, for the magnitude-only data and complex data models yellow, and for all three models green. There were no voxels that were above threshold for both the phase-only data model and the complex data model assigned dark blue. It can be seen that the pink voxels with task related phase changes are below the threshold for the complex data model. A closer inspection of the red voxels reveals that they also exhibit task related phase changes. It can be concluded that the magnitude activation from complex data model with a constant phase strongly biases against voxels with task related phase changes, which was verified by additional simulations (not shown). It was recently shown that voxels containing large vessels exhibit task related changes in both the magnitude and phase whereas voxels with small vessels such as parenchymal tissue only have task related magnitude changes [6].

CONCLUSION

The magnitude-only data, phase-only data, and magnitude activation from complex data with a constant phase models were applied to a real data set. Activation from this complex data model was more focused over the magnitude-only data model and concentrated on voxels without phase changes.

REFERENCES

1. Bandettini, P.M. et al. (1993). Processing strategies for time-course data sets in functional MRI of the human brain. MRM. 30(2):161-173.
2. Rowe, D.B. and Logan, B.R. (2004). A complex way to compute fMRI activation. NeuroImage. 23(3):1078-1092.
3. Rowe, D.B. and Logan, B.R. (2005). Complex fMRI Analysis with unrestricted phase is equivalent to a magnitude-only model. NeuroImage, 24(2):603-606.
4. Rowe, D.B. (2005). Parameter Estimation in the Magnitude-Only and Complex-Valued fMRI Data Models. NeuroImage, 25(4): 1124-1132
5. Logan, B.R. and Rowe, D.B. (2004). An evaluation of thresholding techniques in fMRI analysis. NeuroImage. 22(1):95-108.
6. Menon, R.S., (2002). Postacquisition suppression of large-vessel BOLD signals in high-resolution fMRI. MRM 47(1):1-9.